Facile Preparation of Nylon 6 Nanocomposites Based on Clay Reinforcement and Core-Shell Latex Toughening: Morphology, Properties, and Impact Fracture Behavior

Shuangyue Sun,[1,2] Yadong He,[1] Xiaodong Wang,[1,3] Dezhen Wu[3]

[1]*School of Mechanical and Electrical Engineering, Beijing University of Chemical Technology, Beijing 100029, China*
[2]*North College of Beijing University of Chemical Technology, Sanhe, Hebei Province 065201, China*
[3]*School of Materials Science and Engineering, Beijing University of Chemical Technology, Beijing 100029, China*

Received 26 September 2010; accepted 26 October 2010
DOI 10.1002/app.33662
Published online 22 February 2011 in Wiley Online Library (wileyonlinelibrary.com).

ABSTRACT: This work is focused on a facile route to prepare a new type of nylon 6-based nanocomposites with both high fracture toughness and high strength. A series of nylon 6-matrix blends were prepared via melting extrusion by compounding with poly (methyl methacrylate-*co*-butadiene-*co*-styrene) (MBS) or poly(methyl methacrylate-*co*-methylphenyl siloxane-*co*-styrene) (MSIS) latices as impact modifier and diglycidyl ether of bisphenol-A (DGEBA) as compatibilizer. Layered organic clay was also incorporated into above nylon 6 blends for the reinforcement of materials. Morphology study suggests that the MBS or MSIS latex particles could achieve a mono-dispersion in nylon 6 matrix with the aid of DGEBA, which improves the compatibilization and an interfacial adhesion between the matrix and the shell of MBS or MSIS. High impact toughness was also obtained but with a corresponding reduction in tensile strength and stiffness. A moderate amount of organic clay as reinforcing agent could gain a desirable balance between the strength, stiffness and toughness of the materials, and tensile strength and stiffness could achieve an improvement. This suggests that the combination of organic clay and core-shell latex particles is a useful strategy to optimize and enhance the properties of nylon 6. Morphology observation indicates that the layered organic clay was completely exfoliated within nylon 6 matrix. It is found that the core-shell latex particles and the clay platelets were dispersed individually in nylon 6 matrix, and no clay platelets were present in MBS or MSIS latex particles. So the presence of the clay in nylon 6 matrix does not disturb the latex particles to promote high fracture toughness via particle cavitation and subsequent matrix shear yielding, and therefore, provides maximum reinforcement to the polymer.
 J Appl Polym Sci 121: 541–553, 2011

Key words: nanocomposites; nylon 6; core-shell latex; organic clay; reinforcement

INTRODUCTION

Engineering thermoplastics are attractive materials that have been developed in last decades because of their excellent mechanical properties and chemical integrity at elevated temperatures for extended periods of use.[1,2] Nylon 6 is a well-known engineering thermoplastic used in a wide range of applications because of its excellent combination of good mechanical properties and easy processability.[3,4] However, nylon 6 is a pseudoductile polymer that has a fairly high crack initiation energy but a low crack propagation energy, and so it has a high unnotched impact strength but the low-notched one. With increasing demands for high impact resistant thermoplastics, impact modifiers, such as rubbers are added to nylon 6 for toughening. Various different types of rubbers have been used as very effective impact modifiers, including styrene-ethylene/butylene-styrene block copolymer (SEBS) and/or SEBS grafted with maleic anhydride (SEBS-*g*-MA),[5,6] a maleic anhydride modified ethylene-propylene rubber,[7–9] styrene-acrylic acid copolymer,[10] a maleic anhydride modified ethylene–propylene–diene rubber,[11,12] polyethylene-octene copolymer (POE) and/or POE grafted with maleic anhydride (POE-*g*-MA),[13,14] epoxidized ethylene–propylene–diene rubber,[15] ethylene-acrylic acid copolymer,[16] natural rubber with maleic anhydride,[17] epoxidized natural rubber,[18] acrylonitrile-butadiene copolymer,[19] core-shell impact modifiers,[20,21] and so on. Nylon 6 can be well toughened by melt blending with rubbers, provided that an appropriate rubber particle size, or interparticle distance, is established during mixing and there is adequate adhesion between the nylon 6 and rubber phases.

Actually, the incorporation of rubbers provides a new material with higher fracture toughness relative to the untoughened polymer; nevertheless, completely useful properties are still not acquired due to

Correspondence to: X. Wang (wangxdfox@yahoo.com.cn).
Contract grant sponsor: National Key Technology R&D Program for the 11th Five-year Plan; contract grant number: 2008BAE59B04.

inherent loss in stiffness, modulus, and yield strength because of the low rigidity of the rubber particles. Stiffness and fracture toughness are opposing performance parameters and a better balance is required to develop an efficient material. To overcome this problem, the appropriate addition of reinforcing fillers such as nanoclays and glass fiber into nylon 6 systems can remedy the reduction in Young's modulus and tensile strength of the rubber modified nylon 6 blends and manufacture composites.[22–24] The thermoplastics reinforced with nanoclays or layered silicates have been shown to exhibit enhancements in stiffness, modulus, and strength at low concentrations with minimal loss in toughness. Nylon 6/organic montmorillonite (MMT) nanocomposite was considered as the most successful example of polymer/clay nanocomposites and has been extensively investigated.[25,26] Clays as reinforcing materials for polymers owe to unique intercalation/exfoliation characteristics and their potentially high aspect ratio. Commonly used nanoclays (layered silicates) are exfoliated into platelets with a thickness of 1 nm and lateral dimensions of the order 200–1000 nm and uniformly dispersed in polymer matrix. Hence these particles have an aspect ratio of 200–1000. This high aspect ratio of the clay platelets can be effectively used to improve the stiffness and strength of polymer.[27–29] Moreover, polymer-clay nanocomposites have unique properties when compared with conventional filled polymers. For example, the tensile and flexural strength, Young's and flexural modulus of a nylon 6 clay nanocomposite, with a clay mass fraction of only 5 wt %, show excellent improvement with the impact strength being lowered by only 10 wt %.[26] While for the glass fiber reinforced, rubber-toughened material, the stiffness and strength of material can be much higher than neat nylon 6 if a sufficient amount of glass fiber is used; however, the elongation at break and Izod impact strength of the rubber-toughened thermoplastic is reduced when glass fibers are introduced. Even a small amount of glass fiber (lower than 5 wt %) is sufficient to cause a 50% reduction in Izod impact strength.[24]

In recent years, ternary nanocomposites based on nanoclays as reinforcing fillers and rubbers used as impact modifiers have attracted great attention in both academic and industry to achieve satisfied balanced properties. Chiu et al.[30] evaluated the combined effects of adding the organic clay and maleated metallocene POE impact modifier on nylon 6/clay nanocomposites preparation and their thermal and mechanical properties. In another study, Ahn and Paul[31] investigated the rubber toughening of nylon 6 nanocomposites, and found that the addition of clay affected the dispersion of the rubber phase resulting in larger and more elongated rubber particles. Gonzalez et al.[32] reported that supertough nylon 6/clay nanocomposites could be obtained with addition of 30 wt % SEBS-*g*-MA, and the rubber particle size generally decreased when the MA content of SEBS increased. Lim et al.[33] studied the quasi-static toughness and associate failure mechanisms of nylon 6/organic clay/POE-*g*-MA ternary nanocomposites and analyzed individual effects of organic clay and dispersed rubber particles in the nylon 6 matrix during the deformation and fracture processes. According to Dasari et al.,[34,35] the level of enhancement in fracture toughness of nylon 66-based ternary nanocomposites with organic clay as the reinforcing agent and a soft elastomer, SEBS-*g*-MA, as the toughening agent depends on the capability of different fillers to activate the plastic deformation mechanisms in the matrix and the blending protocol employed.

In this study, we developed a facile one-step melting process for the preparation of nylon 6-based ternary nanocomposites using core-shell lattices as an impact modifiers and organic clay as a reinforcing agent. The core-shell lattices used have a typical core-shell structure for their individual latex particles, which have a glassy shell that can be designed to protect the core during mixing process and a rubbery core acting as an impact modifier for the toughened polymers. The particle size of core-shell lattices, which is set during the synthesis process, can remain after they are dispersed in a polymer matrix. So all agglomerates of these latex particles are readily broken up and their particles are individually dispersed in the matrix, which can ensure the desired particle shape and their uniform dispersion in the matrix phase. It is well known that the core-shell lattices like MBS can impart very high toughness to nylon 6 with the aid of certain diglycidyl ether of bisphenol-A (DGEBA) as compatibilizer.[20,36] Since DGEBA is miscible with the polymethyl methacrylate (PMMA) shell of MBS, which is due to the specific interaction, e.g., hydrogen bonding, formed between these two polymers. In addition, the epoxy groups of DGEBA, as functionalized sites, can react with the terminal amino group in nylon-6. Therefore, DGEBA as a reactive compatibilizer can reduce the interfacial tension, enhance the interfacial adhesion between the latex particles and nylon 6, and suppress the dispersed phase coalescence. Furthermore, nanoclays as a reinforcing agent were added to the core-shell latex toughened nylon 6 blends, and we expected to gain the improvement in strength and modulus so that the decrease in stiffness of rubber-toughened nylon 6 could be remedied. In addition, we also attempt to further extend the fundamental knowledge in understanding the fracture behavior and toughening process for ternary nanocomposites, particularly focusing on their notched impact energy.

EXPERIMENTAL

Materials

The nylon 6 (1013B) used in this study was commercially obtained from UBE Industries, Japan with a number average molecular weight of 25,000. The density of nylon 6 is 1.14 g cm^{-3} while the melting point is around 215–225°C. Two types of core-shell lattices with commercial product names of Kane Ace® M-600 and MR-01 were kindly supplied by Kaneka Chemical, Japan. Kane Ace M-600 is a core-shell structured MBS latex containing a polybutadiene rubbery core with a T_g of −60°C and PMMA plastic shell, and it has a particle diameter of 200–300 nm. Kane Ace MR-01 is a kind of core-shell structured poly(methyl methacrylate-*co*-methylphenyl siloxane-*co*-styrene) (MSIS) lattices having a ploy(methylphenyl siloxane) (PMPS) rubbery core with a T_g of −120°C as well as a PMMA plastic shell, and it has the same particle size range with M-600. DGEBA, EPICLON® 7050 with an epoxide equivalent weight of 1750–2100 g $equiv.^{-1}$ was kindly supplied by Wuxi Bluestar Epoxy, China. Organically modified montmorillonite (OMMT), Nanomer® I.34TCN, with cation ex-change capacity of 90 meq/100 g was obtained from Nanocore, America.

Preparation of blends and nanocomposites

All of the raw materials were dried in a vacuum oven for a minimum of 16 h at 80°C to ensure removal of absorbed water prior to melt compounding. Nylon 6-based blends and nanocomposites were prepared by one-step melting extrusion in a Werner and Pfeiderer ZSK25-WLE twin-screw extruder ($L/D = 30$, $D = 25$ mm), followed by injection molding with a Haitian HFF120 × 2 injection-molding machine. The temperatures of the extruder at three zones of the barrel and at the die were 220, 230, 245, and 235°C, respectively, and the screw speed was 250 rpm. The extruded strings were cooled in a water bath and then pelletized. The pelletized extrudates were dried in a vacuum oven at 85°C overnight and then injection molded into standard tensile (ASTM D638) and Izod impact (ASTM D256) and flexible (ASTM D790) test bars. The injection-molding machine was set with the barrel and mold temperatures of 245 and 60°C, respectively.

Characterization

Mechanical property tests

All test bars were kept in a sealed desiccator under vacuum for 24 h before mechanical property measurements were performed. The tensile and flexible properties were measured with a SANS CMT-4104 universal testing machine using a 10,000 Newton load transducer according to the standards of ASTM D-638 and D-790, respectively. Notched Izod impact strength was measured with a SANS ZBC-1400A impact tester according to ASTM D256. The thickness of the notched Izod impact bars was 1/8 in., and impact energy was 4 J. All the tests were done at room temperature and the values reported reflected an average from five measurements.

Measurement of melt flow index

Melt flow index (MFI) of the samples were measured by using a SANS ZRZ1452 melt flow indexer operating at 230°C and 2.16-kg load according to ASTM D-1238.

X-ray diffraction

X-ray diffraction (XRD) measurements were made directly from organic clay powders. In the case of the nanocomposites, the measurements were carried out using the samples obtained from the injection molded tensile test bars. All these experiments were performed in reflection mode using a Japan Rigaku D/max–r C X-ray diffractometer using Cu Kα radiation ($\lambda = 0.154$ nm) and operated at 40 kV and 20 mA with a scan rate of 1° min^{-1} in a 2θ range of 0.5°–10°.

Scanning electron microscopy

Scanning electron microscopy (SEM) was employed to observe the morphology of the undeformed specimens. The specimens were cryogenically fractured in liquid nitrogen, and then were etched in boiling toluene for 2 h to selectively dissolve the core-shell structured latex particles. The cryogenic fracture surfaces were coated with a thin layer of gold-palladium and the phase morphology was observed in a Hitachi *S*-4700 scanning electron microscope operating at an accelerating voltage of 20 kV. Then, the SEM images were evaluated to determine the dispersion of core-shell structured latex particles in the nylon 6 matrix and the effect of clay layers on the dispersion of these particles in the ternary nanocomposites.

Transmission electron microscopy

The morphologies of the binary blends and ternary nanocomposites were also determined by transmission electron microscopy (TEM) using a Hitachi H-800 transmission electron microscope operating at an accelerating voltage of 200 kV. Ultrathin samples were obtained from molded specimens by microtoming perpendicular to the flow direction using a

diamond knife below the brittle temperature of nylon 6 to maintain the rigidity of the specimens. The microchips were stained using an aqueous solution of OsO_4 over a period of at least 20 min to enhance the phase contrast among the nylon 6, clay, and MBS lattices. The rubber particles appear black in the TEM images. Subsequently the specimens were transferred into a copper grid.

Differential scanning calorimetry

The thermal behaviors of both neat nylon 6 and the nanocomposites were measured by a TA Instruments Q100 differential scanning calorimeter equipped with a thermal analysis data station, operating at a heating rate of 10°C min^{-1} under nitrogen atmosphere. The extruded samples were heated from room temperature to 300°C and held at 300°C for 5 min to eliminate the influence of thermal history, then cooled to 20°C at a rate of 10°C min^{-1}, and a second scan was carried out in a similar manner. The melting temperature (T_m), melting enthalpy (ΔH_m), crystallization temperature (T_c), and crystallization enthalpy (ΔH_c) of nylon 6 and its nanocomposites were determined from DSC measurements.

Thermogravimetric analysis

Thermogravimetric analysis (TGA) was performed in a nitrogen atmosphere using a TA Instruments Q50 thermal gravimetric analyzer. Samples placed in an Alumina crucible, and ramped from 40 to 700°C at a heating rate of 20°C min^{-1} while the flow of nitrogen was maintained at 50 mL min^{-1}.

RESULTS AND DISCUSSION

Morphology

The cryofractured surfaces of the samples were observed to determine the degree of dispersion for the core-shell lattices dispersed in the nylon 6 matrix using SEM as described in the Experimental section. Figure 1 displays the SEM images of these cryofractured surfaces for the nylon 6 nanocomposites containing various amounts of the core-shell lattices, DGEBA, and organic clay. Through a solution etching to remove the core-shell latex particles from the cryofractured surfaces, the holes remained on the surfaces could reflect the dispersion of these latex particles in the matrix. It is observed that both the nylon 6/MBS and nylon 6/MSIS binary blends exhibit the multiporous surfaces with a nonuniformly hole-size distribution as shown in Figure 1(a,b). As introduced in the Kane Ace product brochure, these types of core-shell structured latices have a particle size of around 200 nm. However, it is found that most of the hole sizes are as great as around 3 μm, which are much larger than the latex particles employed in this study. These results indicate that the dispersion of two types of the lattices is actually poor. This appears due to a poor compatibility between nylon 6 and the PMMA shell of MBS or MSIS, which results in an aggregation of these latex particles during the melt blending, and the large holes correspond to the agglomerates of these particles in the matrix. Furthermore, Figure 1 also reveals that the core-shell latices are well dispersed in the nylon 6 matrix when 1 wt % DGEBA is incorporated as a compatibilizer. The addition of 3 wt % DGEBA further improves the dispersion of the lattices, and in this case, it is clearly observed that the most of the MBS or MSIS are monodispersed as individual latex particles as seen in Figure 1(c,d). However, there does not seem to be any substantial change in the dispersion of the latex particles when 5 wt % DGEBA is incorporated. The TEM image for the nylon 6/MBS blend also confirms the homogenous distribution of rubbery particles in the matrix with the aid of compatibilizer as shown in Figure 2, though the TEM observation for the nylon 6/MSIS are infeasible because the rubbery core of MSIS does not contain any double bonds that can be stained. No agglomerates are found in TEM image, as more than 3 wt % DGEBA is added. This is no doubt due to the compatibilizing effect of DGEBA, which actually improves the compatibility between nylon 6 and core-shell lattices and consequently causes a well dispersion of latex particles.

To act as a compatibilizer for nylon 6 and MBS or MSIS, it is critical for DGEBA to be miscible or compatible both with nylon 6 and with two types of lattices. A few reported studies suggested that DGEBA was thermodynamic with PMMA, the shell component of these two lattices. On the other hand, it is well known that that the epoxy group of DGEBA can be reacted with the functional groups within nylon 6 like amino and imino groups. Moreover, the hydrogen bonding may also be generated between these two polymers. This compatibilizing procedure is schematically depicted in Figure 3. In this case, the role of DGEBA as compatibilizer for nylon 6/core-shell lattices is now clear from the morphological observation. Incorporation of DGEBA into the binary blends can reduce the interfacial tension and improve the interfacial adhesion between nylon 6 and core-shell lattices through the chemical and physical bonding, and results in a homogenous dispersion of core-shell lattices in the matrix.

For the nylon 6/core-shell latex/DGEBA/clay nanocomposites, it is notable that the latex particles still distribute homogeneously when 5 wt % clay is added, and no aggregated particles can be observed (see Fig. 4). This suggests that the presence of clay did not seem to modify the dispersion of core-shell

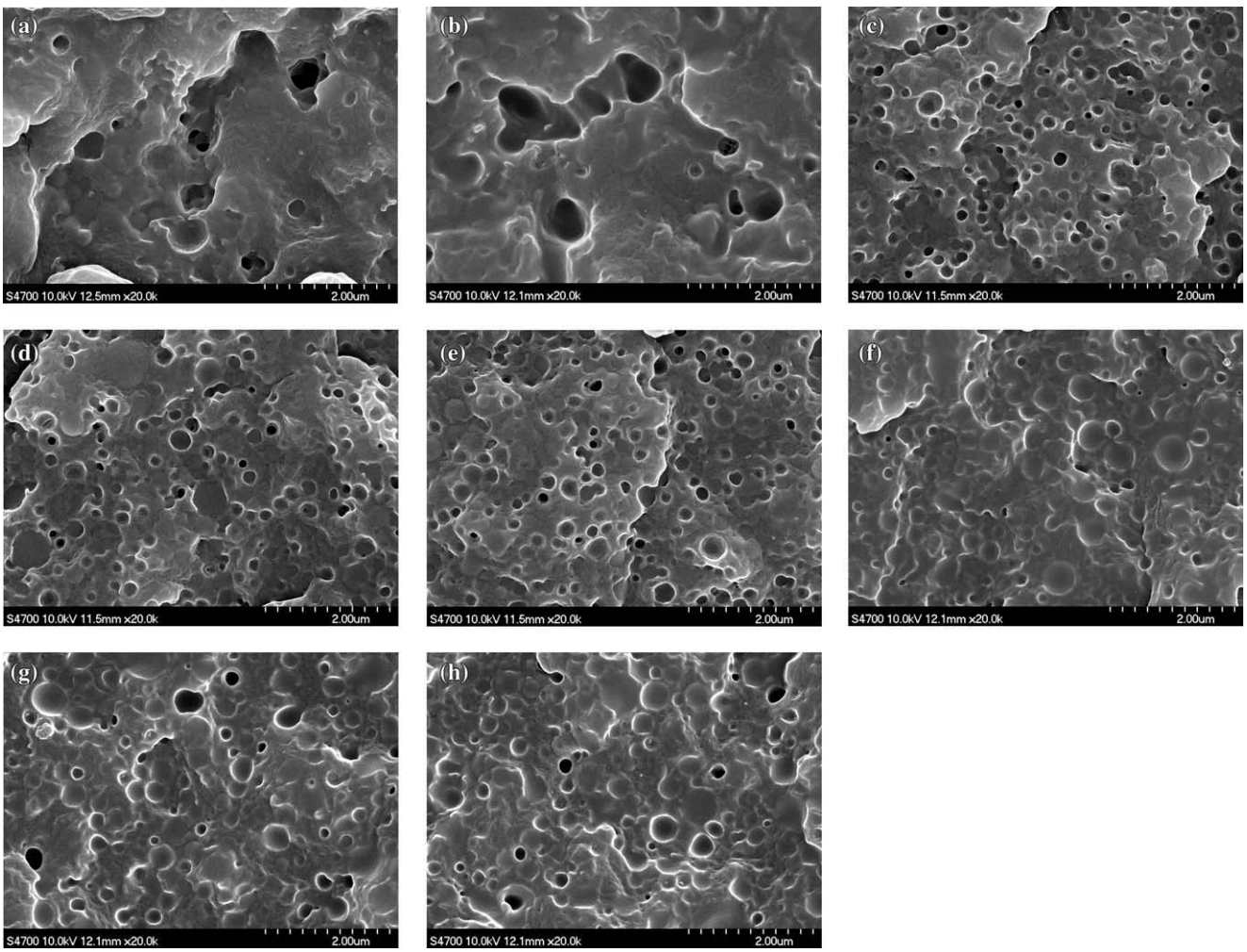

Figure 1 SEM images of the fracture surface of nylon 6/core-shell latex/DGEBA blends at different weight ratios: (a) 85/15(MBS), (b) 85/15(MSIS), (c) 85/15(MBS)/1, (d) 85/15/3, (e) 85/15/5, (f) 85/15(MSIS)/1, (g) 85/15/3, and (h) 85/15/5.

lattices. Figure 5 shows the TEM images of the nylon 6/core-shell latex/DGEBA/clay nanocomposites, in which the dark lines represent the intersection of clay layers while the gray background corresponds to the nylon 6 matrix. It also should be mention that, for the nanocomposites contain MBS, the dark particles in Figure 5(a,b) represent the OsO_4-stained polybutadiene core of MBS, and however, there are no phenomenon found in the nanocomposites containing MSIS because the MSIS does not contain any groups for stain. These TEM images exhibit an appreciable level of clay exfoliation. It can be seen that the clay layers are randomly distributed and uniformly dispersed in nylon 6 matrix. The exfoliated clay platelets as well as a fraction of partially swollen stacks of clay are found in nylon 6 matrix.

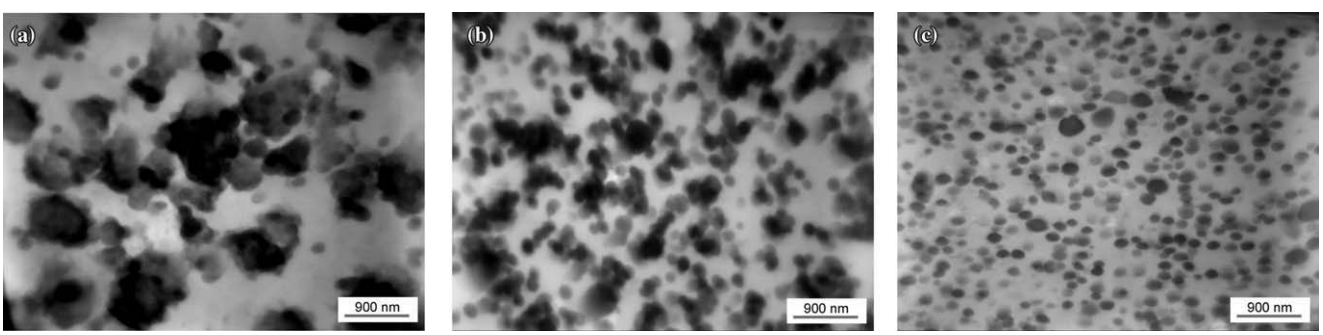

Figure 2 TEM images of the fracture surface of nylon 6/MBS/DGEBA blends at different weight ratios: (a) 85/15, (b) 85/15/1, and (c) 85/15/3.

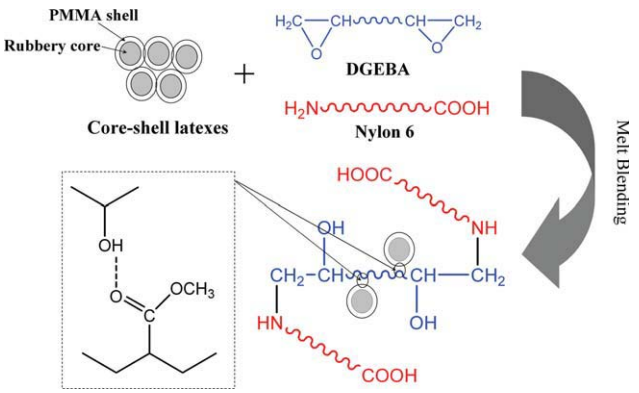

Figure 3 Schematic process of the compatibilizing effect of DGEBA on nylon 6/core-shell latex blends. [Color figure can be viewed in the online issue, which is available at wileyonlinelibrary.com.]

It is well known that the *in situ* polymerization reaches good exfoliation of the clay platelets due to an intercalation of the monomer in the nanostructure clay layers. There are lots of actual studies in the field of *in situ* polymerization of nylon 6 focusing on the synthesis via hydrolytic polymerization.[37,38] The dispersion of the organic clay may be optimized compared to standard melt compounding processes due to the intercalation with the monomer and a consequent shear energy input in the twin-screw extruder. As a result of the homogeneously dispersed clay, the mechanical properties should be significantly increased. Although *in situ* polymerization is aimed at obtaining a nylon matrix strongly bonded to the delaminated clay platelets, it is clear that from a process-engineering point of view, many challenging aspects (e.g., simple and high efficiency) are still attributed to melt blending technique. On the other hand, the clay layers are easily exfoliated by nylon 6 molecular chains because of their high polarity when the melt compound technique is employed, and a good dispersion of clay can be achieved like this study. It is well established that surface modification of the hydrophilic clay layers with organic surfactants expands the intragalleries of clay layers thus decreasing the electrostatic interactions between adjacent clay layers and rendering good compatibility between polymer chains and organic clay layers. Moreover, the organic modification also resulted in an increase in basal spacing of clays. The larger initial layer spacing may lead to easier exfoliation since layer–layer attraction is reduced. It is implied that diffusion of polymer chains inside clay galleries is less hindered due to increased spacing and ultimately leads to improved exfoliation. In addition, clay layers are not observed in the rubber domains because the rubber core of the core-shell lattices is well protected by the plastic PMMA shell. Therefore, even if it cannot be excluded that a minor amount of clay was incorporated in the PMMA phase, it may be assumed that almost all clay layers were contained in the nylon 6 matrix.

Melt flow index

MFI measurements provide an approximate characterization of the melt viscosity at the conditions that exist inside the extruder. Table I shows the MFI values of nylon 6 and its nanocomposites. The blends of nylon 6 with two types of core-shell lattices exhibit lower values of MFI than pure nylon 6, probably because of a change in the flow mechanism due to the addition of high viscous core-shell lattices. It can be seen that the incorporation of DGEBA as compatibilizer into nylon 6/core-shell latex blends results in a remarkable decrease in MFI values. This is no doubt due to the results of the compatibilizing reaction between the nylon 6 and DGEBA as well as the enhanced interaction between the core-shell

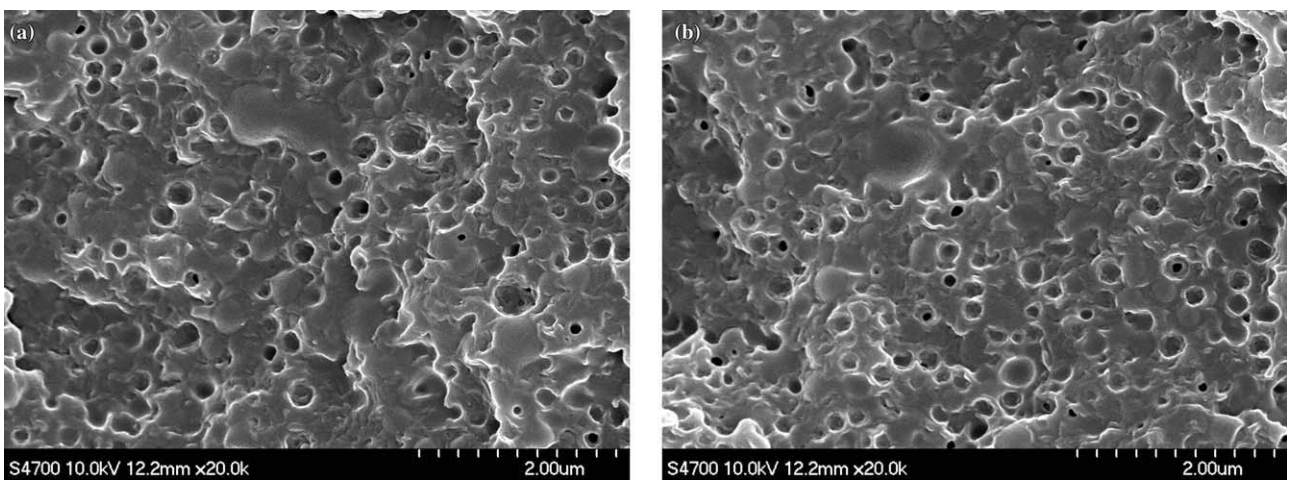

Figure 4 SEM images of the fracture surface of nylon 6/core-shell latex/DGEBA/clay nanocomposites at different weight ratios: (a) 85/15(MBS)/3/5, and (b) 85/15(MSIS)/3/5.

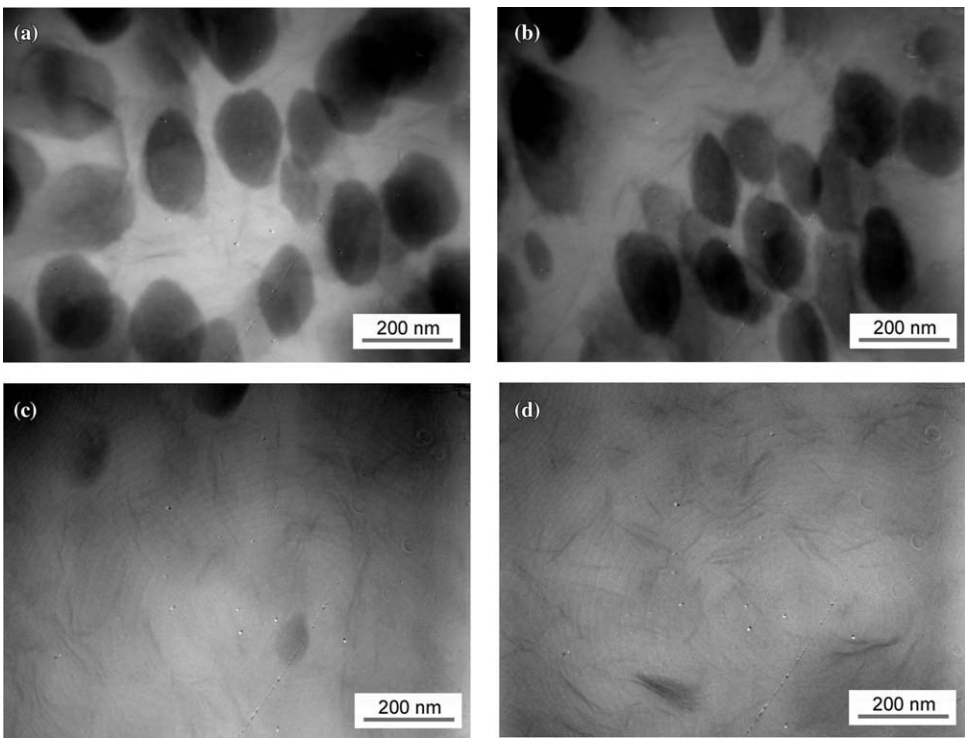

Figure 5 TEM images of the fracture surface of nylon 6/core-shell latex/DGEBA/clay nanocomposites at different weight ratios: (a) 85/15(MBS)/3/3, (b) 85/15/3/5, (c) 85/15(MSIS)/3/3, and (d) 85/15/3/5.

lattices and DGEBA through the hydrogen bonding. Furthermore, a much more significant reduction in the MFI values of the nylon 6 nanocomposites has been observed in the presence of clay. This may be attributed to the interaction between the amino groups of organic modifier on the clay and amide/imino groups within the nylon 6 via hydrogen bonding. In addition, individual clay layers with high aspect ratio are dispersed homogenously in the nylon 6 matrix. This leads to a high contact surface area and gives rise to a strong interaction between the clay and nylon 6 matrix. Thus, the melt viscosities of the nylon 6 nanocomposites are improved greatly.

X-ray diffraction

Figure 6 presents typical XRD patterns of unmodified clay, organically modified clay and the nylon 6 nanocomposites containing 5 wt % organic clay. The pattern of the unmodified clay displays a characteristic diffraction (001) peak at $2\theta = 7.08^\circ$, which corresponded to a basal spacing of 1.32 nm according to the Bragg's low. For organically modified clay, the diffraction corresponding to *d*-spacing appears at $2\theta = 4.87^\circ$. The characteristic peak of organic clay shifts to a lower angle corresponding to an increase in the

TABLE I
The MFI Values of Nylon 6 and Its Nanocomposites

Composition (wt %)					
Nylon 6	MBS	MSIS	DGEBA	Clay	MFI (g/10 min)
100	–	–	–	–	38.44
85	15	–	–	–	29.71
85	–	15	–	–	28.35
85	15	–	3	–	9.62
85	–	15	3	–	8.21
85	15	–	3	5	1.85
85	–	15	3	5	1.43

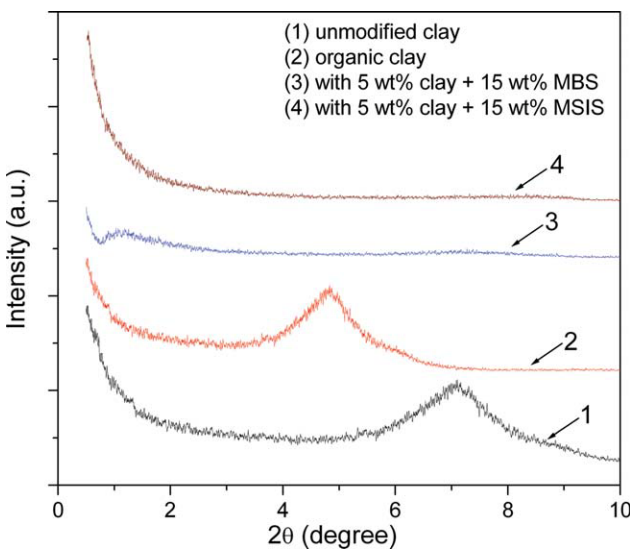

Figure 6 XRD patterns of clay and nylon 6/clay nanocomposites. [Color figure can be viewed in the online issue, which is available at wileyonlinelibrary.com.]

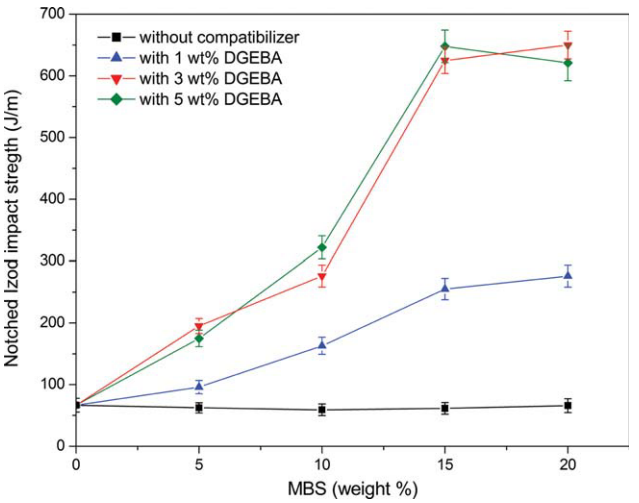

Figure 7 Notched Izod impact strength of nylon 6 blends containing various amounts of MBS and DGEBA. [Color figure can be viewed in the online issue, which is available at wileyonlinelibrary.com.]

d-spacing to 1.86 nm, which indicates that a periodic and swollen intercalated structure is formed when the surfactant was intercalated into the gallery of clay layers. However, when organic clay was incorporated into nylon 6/MBS or MSIS blends and the nanocomposites were obtained through melting extrusion, the characteristic peak of the organic clay disappeared between 1° and 10° in their XRD patterns. The absence of this characteristic diffraction suggests that the clay layers are completely exfoliated in the nylon 6 matrix. This result is consistent with the previous observation of the TEM images, in which the exfoliated clay platelets considered as separated dark lines were homogeneously distributed in the nylon 6 matrix. However, the presence of an intercalated clay structure could not be fully excluded, as these two nanostructures usually coexist in the morphologies of all the polymer/clay nanocomposites.[39] The relative proportion of intercalated and exfoliated species increased with the increase of clay content.[40] It has been documented that the exfoliated structure is the dominant population when the clay content is lower than 5 wt %. Whereas above this level, a mixture of intercalated and exfoliated nanostructures is usually formed.[25,41]

Mechanical properties

To investigate the compatibilizing effect of DGEBA on the impact resistance of nylon 6/core-shell latex blending system, the notched Izod impact strength of nylon 6 and its blends containing various amount of MBS, MSIS, and DGEBA was first evaluated and shown in Figures 7 and 8. It can be found that the binary blends of nylon 6 with either MBS or MSIS are almost as brittle as pure nylon 6. This means that, when the core-shell lattices as impact modifiers were introduced into nylon 6, the impact toughness was not improved significantly as expected. Even if the content of MBS was increased up to 20 wt %, the blends only showed a slight increase in Izod impact value. However, the incorporation of 20 wt % MSIS almost resulted in a decrease in impact strength. The overall variation trends of toughness against the MBS or MSIS content suggest that the core-shell lattices cannot toughen nylon 6 effectively if they are used solely. This is absolutely due to the poor dispersion of the core-shell latex particles as discussed in previous morphology investigation. It has been known that nylon 6 is immiscible or incompatible with the PMMA shell of two types of core-shell lattices, which may result in a poor interfacial adhesion between two polymers, and thus the phase separation between the nylon 6 matrix and core-shell lattices. In addition, it is also notable that the nylon 6/MSB blends show somewhat higher levels of toughness than nylon 6/MSIS ones, which is attributed to the fact that the rubbery core of MBS (i.e., PB) is more elastic than that of MSIS (i.e., PMPS).

As reported previously,[20,36,42] the nylon materials can be toughened by introduction of core-shell structured lattices dispersed with the aid of small amounts of compatibilizer. In this study, a one-step melt-mixing protocol of nylon 6 with MBS or MSIS, and DGEBA should give the greatest opportunity for this compatibilizer to play its proposed function as an interracially acting dispersant. It is as expected that the incorporation of DGEBA reduces a ductile-brittle transition of nylon 6/core-shell latex blending system and improves the impact strength with increasing the loading of core-shell lattices. The best impact resistance is achieved when the DGEBA

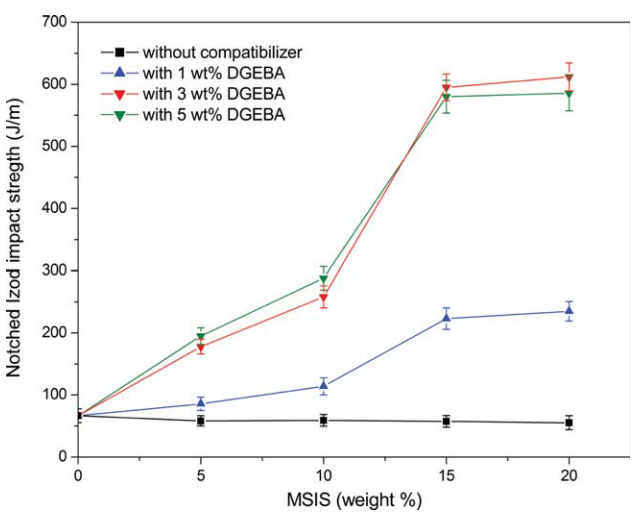

Figure 8 Notched Izod impact strength of nylon 6 blends containing various amounts of MSIS and DGEBA. [Color figure can be viewed in the online issue, which is available at wileyonlinelibrary.com.]

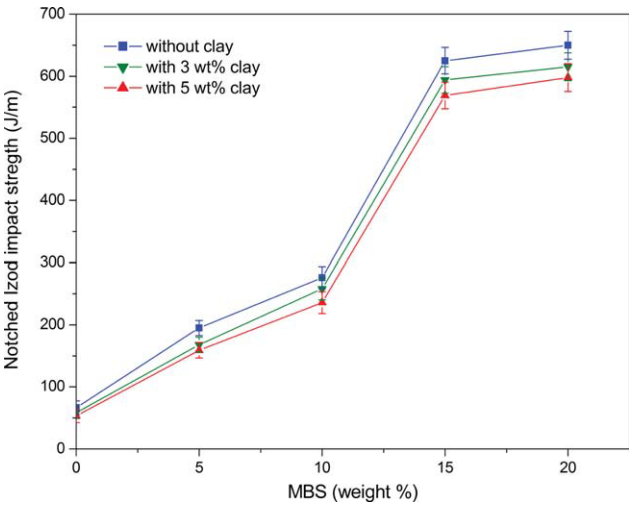

Figure 9 Notched Izod impact strength of nylon 6 nanocomposites containing 3 wt % DGEBA and various amounts of clay and MBS. [Color figure can be viewed in the online issue, which is available at wileyonlinelibrary.com.]

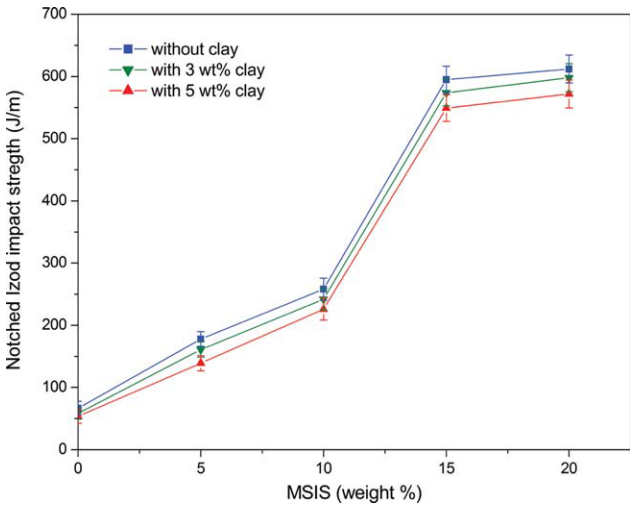

Figure 10 Notched Izod impact strength of nylon 6 nanocomposites containing 3 wt % DGEBA and various amounts of clay and MSIS. [Color figure can be viewed in the online issue, which is available at wileyonlinelibrary.com.]

content is in the range of 3–5 wt %, and these compositions have been shown to have a good dispersion of core-shell latex particles in the matrix as confirmed by the previous SEM and TEM studies. This represents an optimal compatibilizing effect of DGEBA relative to the other two components. However, since the DGEBA itself is a rigid polymer, beyond this range, the blends containing too much compatibilizer can increase their rigidity, and consequently result in the brittleness of material. It also appears that the blends containing 15 wt % core-shell lattices and 3 wt % DGEBA seem to be the optimal composition for the further study when taking into consideration of the balance of toughness and stiffness.

The impact toughness of nylon 6 nanocomposites containing various amount of clay and core-shell lattices was also investigated using the Izod impact test, and the results are shown in Figures 9 and 10. A slight reduction in impact strength of the nanocomposites could be observed when the clay was introduced. This can be attributed to the immobilization of the nylon 6 molecular chains by the clay layers, which limited their ability to adapt to the deformation and make the material more brittle. In addition, each clay platelet or stack of clay layers was the site of stress concentration and could act as a micro crack initiator. It is noteworthy that the ductile-brittle mode of fracture transition is still visible, and a significant toughening effect is maintained even at 5 wt % clay loading. Although the increase of clay loading can continuously deteriorate the toughness of the nanocomposites, the Izod impact strength values of the nanocomposites with 15 wt % MSB or MSIS, and 5 wt % clay still remain at the level of almost ten times as much as that of pure nylon 6, which can evidently be considered as the "supertough" materials.

Table II shows the influence of clay loading on the tensile and flexural properties of nylon 6 and its

TABLE II
Tensile and Flexural Properties of Nylon 6 and Its Nanocomposites

Composition (wt %)					Tensile strength (MPa)	Young's modulus (MPa)	Elongation at break (%)	Flexural strength (MPa)
Nylon 6	MBS	MSIS	DGEBA	Clay				
100	–	–	–	–	69.9 ± 2.1	1854 ± 62	82.8 ± 4.2	56.5 ± 3.3
97	–	–	–	3	74.5 ± 2.4	2218 ± 75	47.9 ± 2.1	57.9 ± 2.9
95	–	–	–	5	78.4 ± 2.3	2725 ± 103	22.3 ± 1.6	59.3 ± 3.5
85	15	–	–	–	55.2 ± 1.7	1427 ± 47	75.4 ± 3.9	46.2 ± 2.4
85	–	15	–	–	56.75 ± 1.9	1483 ± 42	71.6 ± 4.4	48.3 ± 2.3
85	15	–	3	–	58.48 ± 1.4	1492 ± 51	124.9 ± 5.1	49.0 ± 2.5
85	–	15	3	–	59.92 ± 1.6	1528 ± 63	118.5 ± 4.7	50.7 ± 3.3
85	15	–	3	3	62.25 ± 1.8	1697 ± 67	65.2 ± 4.3	51.8 ± 2.8
85	–	15	3	3	62.38 ± 2.2	1725 ± 76	62.9 ± 3.7	52.5 ± 3.2
85	15	–	3	5	63.79 ± 2.3	1807 ± 73	40.8 ± 2.2	53.4 ± 2.7
85	–	15	3	5	64.52 ± 2.1	1814 ± 94	41.7 ± 2.3	55.3 ± 2.9

nanocomposites. It is evident that, while the core-shell lattices toughen nylon 6 effectively under the compatibilization with DGEBA, both the tensile and flexural strength of the blends tend to decrease, whereas the elongation at break substantially increases. This is possibly due to the elastomeric nature of the core-shell lattices. As expected, the tensile and flexural strength, and Young's moduli are significantly improved when clay is incorporated into nylon 6. It is notable that, for the core-shell latex toughened nylon 6 systems, the incorporation of clay considerably enhances the tensile and flexural properties compared to their corresponding blends without clay. This is due to the availability of the large aspect ratio and surface area of clay layers, over which load can be transferred to the nano-reinforcement.[32,43,44] There is also a constraining effect of these layers on molecular motion of polymer chains due to the strong interaction between polymer molecular chains and the surface of exfoliated clay platelets. The presence of 5 wt % clay can provide 90% enhancement in the tensile strength of nylon 6. Based on above results, it is feasible to maintain a suitable balance between the toughness and stiffness of nanocomposites through controlling of the amount of core-shell lattices and clay.

In summary, the appropriate rubber particle size or interparticle distance plays a key role in toughening of plastic materials as suggested by Wu.[45] The lower and upper limits of the weight-average diameter of rubber particles were shown to be 0.1 and 1 μm for nylon 6 by Oshinski et al.[8] In nylon 6/core-shell latex binary blends, the core-shell latex particles with a predetermined particle diameter of 200–300 nm can be dispersed individually in nylon 6 matrix with the aid of DGEBA. It is noted that under impact condition, the core-shell latex particles appear to cavitate. The presence of the core-shell lattices in the nylon 6 matrix initiates a localized energy-absorbing mechanism from many sites rather than from a few isolated ones, in which nylon 6 as a pseudoductile polymer can initiate cavitation as well as promote additional shear yielding during fracture process with relatively higher crack initiation energy but with a low crack propagation energy. The elastic restraint was partially relieved through core-shell particles cavitation and hence the matrix material between the voids was able to shear yield to some extent. Once shear deformation of the voided matrix material was extend, the thus the impact energy can be dissipated by the matrix. A similar observation was reported by Ahn and Paul,[31] rubber particles dispersed within a neat nylon 6 matrix increase toughness via cavitation which relieves the triaxial stress state ahead of the advancing crack trip and allows the nylon 6 matrix to shear yielding and thereby dissipate more energy and enhance toughness. Newman and Strella[46] also found that the principal function of rubber particles is to produce sufficient triaxial tension in matrix so as to increase the local free volume and, hence, the shear yielding. It can be seen that the addition of clay into nylon 6/core-shell lattices blend decreased its impact toughness, but enhanced its tensile and flexural strength, and Young's moduli. The reduction in impact toughness could be attributed to the immobilization of the macromolecular chains by the clay layers, which limited their ability to adapt to the deformation and make plastic deformation of the polymer matrix more small.[47] On the contrary, because with no clay layers in the rubber phase, core-shell latex particles can easily cavitate and promote matrix plastic deformation. So compared with nylon 6/core-shell latex binary blends, the impact toughness of nylon 6/core-shell latex/clay ternary blends was not drastically decreased. The improvement in strength and stiffness may be due to the reinforcement effect of the rigid clay and the constraining effect of clay platelets on molecular motion of polymer molecular chains.[48]

Thermal properties

The melting and crystallization behaviors of nylon 6 and its nanocomposites were studied by DSC, and Figure 6 illustrates the heating and cooling thermograms of these samples, in which all of the plots shown there are normalized by weight and shifted vertically for clarity. The thermal parameters obtained from the DSC analysis are summarized in Table III. From Figure 11(a), one may observe a main melting peak appearing at 220.1°C, which is associated with melting of the α-form crystals of pure nylon 6.[49,50] It can also be seen that there is a much lower endothermic peak at about 215°C as a shoulder of T_m, which is related to the melting of the less stable γ-form crystals of nylon 6.[49,50] These indicate that α-crystals represent the dominant crystalline phase along with the trivial γ-ones in the pure nylon 6. For the nylon 6/MBS or MSIS binary blends, both the shapes of their thermograms and their T_ms and ΔH_ms almost do not change, which indicates that the presence of core-shell lattices does not affect the structure and stability of the crystals formed as well as the crystallinity of nylon 6 due to the incompatibility of two components. However, the incorporation of DGEBA as compatibilizer results in a substantial shift of the main melting peaks towards lower temperature. It is easily understood that DGEBA is reactive with nylon 6, which may restrain the mobility of the molecular chains of nylon 6, and thus interfere with the crystallization of the nylon 6 phases. As a result, the T_ms and ΔH_ms are reduced slightly (see Table III). It is noteworthy

TABLE III
Thermal Parameters of Nylon 6 and its Nanocomposites Obtained from DSC and TGA Measurements

Sample code	Composition (wt %)					T_m (°C)		ΔH_m (J g^{-1})	T_c (°C)	ΔH_c (J g^{-1})	Temperature at 10 % weight loss (°C)	Temperature at rapid weight loss (°C)	Char residue (%)
	Nylon 6	MBS	MSIS	DGEBA	Clay	α-crystal	γ-crystal						
1	100	–	–	–	–	219.8	210.7	163.5	179.6	128.6	430.5	469.7	1.19
2	85	15	–	–	–	219.1	210.8	162.1	180.1	121.4	415.2	456.2	2.04
3	85	–	15	–	–	219.3	210.5	163.2	181.9	122.8	415.9	456.4	2.16
4	85	15	–	3	–	217.1	209.5	159.4	183.4	96.3	–	–	–
5	85	–	15	3	–	216.8	209.3	156.7	183.2	92.5	–	–	–
6	85	15	–	3	5	214.9	208.1	154.2	187.5	94.2	416.3	457.1	3.65
7	85	–	15	3	5	214.6	208.0	152.9	187.3	88.4	–	–	–

that, for the nylon 6/core-shell latex/clay nanocomposites under the compatibilization of DGEBA, the magnitude of the melting peak corresponding to the γ-form crystals of nylon 6 is significantly enhanced while that of the α-form ones weaken, and meanwhile there is a slight shift of the melt peak of nylon 6/clay binary nanocomposite towards much lower temperature. This suggests that the addition of clay into pure nylon 6 induces a crystal phase transformation from α-form to γ-one due to heterogeneous nucleation effect of the exfoliated clay platelets, and may probably destroy the perfection of the α-form crystals simultaneously, which also results in a slight decrease in the T_m and ΔH_m of nylon 6/clay binary nanocomposites.[31]

On the other hand, a single exothermic crystallization peak is observed in the cooling scans of all the samples as shown in Figure 11(b). As listed in Table III, the T_cs and ΔH_cs of the nylon 6/MSB or MSIS binary blends are similar to those of pure nylon 6 as a result of incompatibility of the two components. However, the addition of DGEBA into the blends drastically causes an increase in T_c but a decrease in ΔH_c. It is clear that the reaction of DGEBA with nylon 6 can retard the crystallization of nylon 6 phases in the blends, and further reduce the degree of crystallinity. Furthermore, when clay is incorporated into the ternary blends, the presence of clay also leads to a further decrease in the T_c of nylon 6 phases. This indicates that the dispersed clay layers retard the mobility of nylon 6 chains and thus hinder the crystallization of nylon 6 phases.[31,51] In addition, a decrease in ΔH_c is also observed for nylon 6 nanocomposites. It is implied that the added

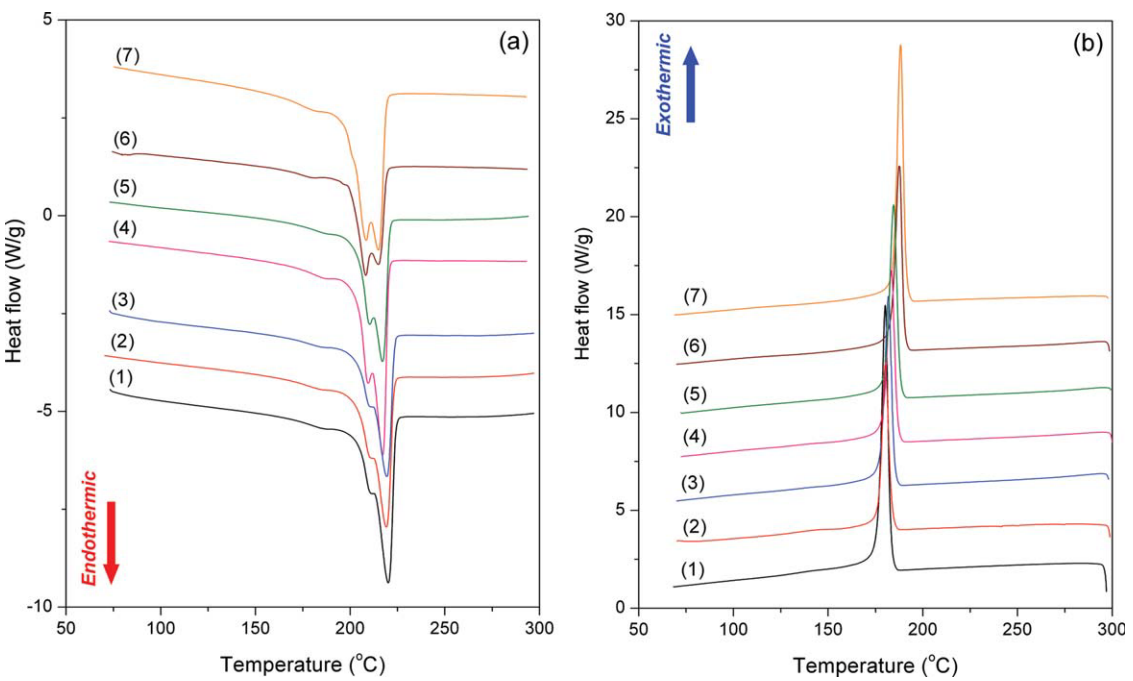

Figure 11 DSC thermograms of nylon 6 and its nanocomposites: (a) heating curves and (b) cooling curves; the curve number corresponds to the sample code and composition listed in Table III. [Color figure can be viewed in the online issue, which is available at wileyonlinelibrary.com.]

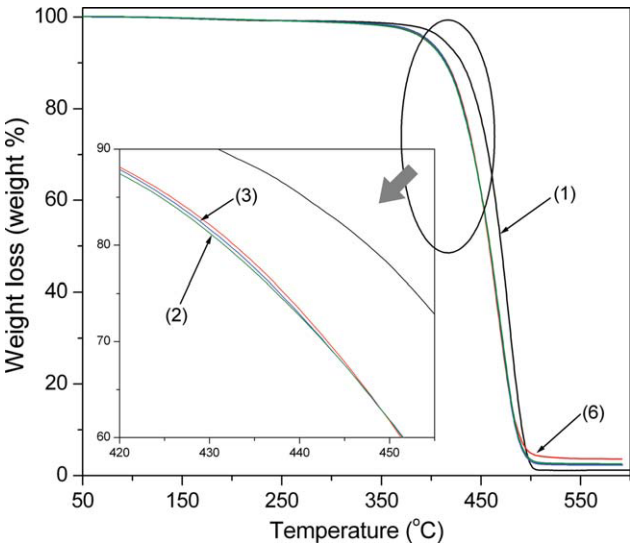

Figure 12 TGA thermograms of nylon 6/core-shell latex/DGEBA/clay nanocomposites; the curve number corresponds to the sample code and composition listed in Table III. [Color figure can be viewed in the online issue, which is available at wileyonlinelibrary.com.]

clay can play a role of effective nucleating agent in the nanocomposites, and consequently deteriorated the perfection of the crystalline structure of nylon 6, leading to a reduction in the degree of crystallinity.

The thermal degradation behaviors of nylon 6 and its composites were evaluated by TGA. Figure 12 presents their TGA thermograms, and the corresponding thermal parameters are also summarized in Table III. It is observed that all of the samples undertake a slight weight loss between 50 and 115°C as a result of water volatilization. Pure nylon 6 keeps mass stable until 235°C, and then begins to experience a significant weight loss as a result of the thermal decomposition of its molecular chains. This thermal degradation continuously performs until 485°C. For the nylon 6/MBS blend, the characteristic temperatures both at 10% weight loss and at rapid weight loss decrease, which is probably attributed to the poor thermal stability of core-shell latex. It is also seen that the incorporation of DGEBA can slightly improve the decomposition temperature due to the compatibilizing effect. However, the nanocomposite of nylon 6/MBS/DGEBA with clay also exhibits a lower degradation temperature but a higher char residue in comparison with those of pure nylon 6. It is concluded that the thermal stability of the nanocomposites is dominated by the core-shell lattices in the nylon 6 matrix.

CONCLUSIONS

Nylon 6/core-shell latex blends and nylon 6/core-shell latex/clay nanocomposites were prepared by a one-step melt compounding technique using corotating twin-screw extruder. DGEBA as compatibilizer was incorporated into above blends and nanocomposites to enhance the dispersibility of core-shell lattices in nylon 6 matrix, and consequently conduct a significant toughening effect. SEM, TEM and XRD results revealed that the presence of organic clay did not produce any apparent effect on the dispersion of core-shell lattices in the nylon 6 matrix, in which organic clay layers completely exfoliated and core-shell latex particles were individually dispersed. The absence of clay in the core-shell lattices allows cavitation of the latex particles triggering substantial yielding of the voided matrix material. So the incorporation of organic clay into the nylon 6/core-shell latex binary blends enhanced strength, stiffness, but slightly reduced impact toughness. The addition of both core-shell lattices and organic clay into nylon 6 produced the balanced properties between strength, stiffness, and toughness. The DSC result showed an evident phase transformation from α-form to γ-form crystals, which indicated that the introduction of organic clay into the polymer matrix had a strong heterophase nucleation effect and deteriorated the perfection of the crystalline structure of nylon 6, leading to a reduction in the degree of crystallinity. The TGA data confirmed the slight thermal stability decline of nylon 6 after adding core-shell lattices and organic clay.

References

1. Lyons, J. S. Polym Test 1998, 17, 237.
2. Segatelli, M. G.; Yoshida, I. V. P.; Gonçalves, M. C. Compos Part B 2010, 41, 98.
3. Unal, H.; Mimaroglu, A. J Reinf Plast Compos 2004, 23, 461.
4. Kumar, A.; Ramanaiah, B. V.; Ray, A. R. Polym Plast Technol Eng 2006, 45, 1039.
5. Huang, J. J.; Keskkula, H.; Paul, D. R. Polymer 2004, 45, 4203.
6. Kayano, Y.; Keskkula, H.; Paul, D. R. Polymer 1997, 38, 1885.
7. Oshinski, A. J.; Keskkula, H.; Paul, D. R. Polymer 1996, 37, 4891.
8. Oshinski, A. J.; Keskkula, H.; Paul, D. R. Polymer 1996, 37, 4909.
9. Harada, T.; Carone E., Jr.; Kudva, R. A.; Keskkula, H.; Paul, D. R. Polymer 1999, 40, 3957.
10. Lu, M.; Keskkula, H.; Paul, D. R. Polym Eng Sci 1994, 34, 33.
11. Vieira, I.; Severgnini, V. L. S.; Mazera, D. J.; Soldi, M. S.; Pinheiro, E. A. Polym Degrad Stabil 2001, 74, 151.
12. Wang, C.; Su, J. X.; Li, J.; Yang, H.; Zhang, Q.; Du, R. N.; Fu, Q. Polymer 2006, 47, 3197.
13. Premphet-Sirisinha, K.; Chalearmthitipa, S. Polym Eng Sci 2003, 43, 317.
14. Huang, J. J.; Paul, D. R. Polymer 2006, 47, 3505.
15. Wang, X. H.; Zhang, H. X.; Jiang, W.; Wang, Z. G.; Liu, C. H.; Liang, H. J.; Jiang, B. Z. Polymer 1998, 39, 2697.
16. Valenza, A.; Visco, A. M.; Acierno, D. Polym Test 2002, 21, 101.
17. Carone, E., Jr.; Kopacak, U.; Goncalves, M. C.; Nunes, S. P. Polymer 2000, 41, 5929.
18. Tanrattanakul, V.; Sungthong, N.; Raksa, P. Polym Test 2008, 27, 794.
19. Scaffalo, R.; La Mantia, F. P.; Bertani, R.; Sassi, A. Macromol Symp 2003, 202, 67.

20. Lu, M.; Keskkula, H.; Paul, D. R. J Appl Polym Sci 1996, 59, 1467.
21. Yu, Z. Z.; Ou, Y. C.; Qi, Z. N.; Hu, G. H. J Polym Sci Part B Polym Phys 1998, 36, 1987.
22. Hassan, A.; Othman, N.; Wahit, M. U.; Wei, L. J.; Rahmat, A. R.; Ishak, Z. A. M. Macromol Symp 2006, 239, 182.
23. Njuguna, J.; Pielichowski, K.; Desai, S. Polym Adv Technol 2008, 19, 947.
24. Laura, D. M.; Keskkula, H.; Barlow, J. W.; Paul, D. R. Polymer 2000, 41, 7165.
25. Fornes, T. D.; Hunter, D. L.; Paul, D. R. Polymer 2004, 45, 2321.
26. Swain, S. K.; Isayev, A. I. J Appl Polym Sci 2009, 114, 2378.
27. Cho, J. W.; Paul, D. R. Polymer 2001, 42, 1083.
28. Tjong, S. C.; Bao, S. P. Compos Sci Technol 2007, 67, 314.
29. Fu, S. Y.; Feng, X. Q.; Lauke, B.; Mai, Y. W. Compos Part B 2008, 39, 933.
30. Chiu, F. C.; Lai, S. M.; Chen, Y. L.; Lee, T. H. Polymer 2005, 46, 11600.
31. Ahn, Y. C.; Paul, D. R. Polymer 2006, 47, 2830.
32. González, I.; Eguiazábal, J. I.; Nazábal, J. Compos Sci Technol 2006, 66, 1833.
33. Lim, S. H.; Dasari, A.; Yu, Z. Z.; Mai, Y. W.; Liu, S. L.; Yong, M. S. Compos Sci Technol 2007, 67, 2914.
34. Dasari, A.; Yu, Z. Z.; Mai, Y. W. Polymer 2005, 46, 5986.
35. Dasari, A.; Yu, Z. Z.; Yang, M.; Zhang, Q. X.; Xie, X. L.; Mai, Y. W. Compos Sci Technol 2006, 66, 3097.
36. Wang, X. D.; Li, H. Q. J Appl Polym Sci 2000, 77, 24.
37. Rothe, B.; Elas, A.; Michaeli, W. Macromol Mater Eng 2009, 294, 54.
38. Boussia, A. C.; Damianou, Ch. C.; Vouyiouka, S. N.; Papaspyrides, C. D. J Appl Polym Sci 2010, 116, 3291.
39. Haq, M.; Burgueño, R.; Mohanty, A. K.; Misra, M. Compos Part A 2009, 40, 540.
40. Samyn, F.; Bourbigot, S.; Jama, C.; Bellayer, S.; Nazare, S.; Hull, R.; Castrovinci, A.; Fina, A.; Camino, G. Eur Polym Mater 2008, 44, 1642.
41. Ranade, A.; D'Souza, N. A.; Gnade, B. Polymer 2002, 43, 3759.
42. Gaymans, R. J.; van der Werff, J. W. Polymer 1994, 35, 3658.
43. Kiliaris, P.; Papaspyrides, C. D. Prog Polym Sci 2010, 35, 902.
44. Usuki, A.; Kojima, Y.; Kawasumi, M.; Okada, A.; Fukushima, Y.; Kurauchi, T. J Mater Res 1993, 8, 1179.
45. Wu, S. Polymer 1985, 26, 1855.
46. Newman, S.; Strella, S. J Appl Polym Sci 1965, 9, 2297.
47. Contreras, V.; Cafiero, M.; Da Silva, S.; Rosales, C.; Perera, R.; Matos, M. Polym Eng Sci 2006, 46, 1111.
48. Yu, Z. Z.; Yan, C.; Yang, M.; Mai, Y. W. Polym Int 2004, 53, 1093.
49. Varlot, K.; Reynaud, E.; Kloppfer, M. H.; Vigier, G.; Varlet, J. J Polym Sci Part B Polym Phys 2001, 39, 1360.
50. Li, T. C.; Ma, J. H.; Wang, M.; Tjiu, W. C.; Liu, T. X.; Huang, W. J Appl Polym Sci 2007, 103, 1191.
51. Ma, C. C. M.; Kuo, C. T.; Kuan, H. C.; Chiang, C. L. J Appl Polym Sci 2003, 88, 1686.